# Apatinib enhances the radiosensitivity of the esophageal cancer cell line KYSE-150 by inducing apoptosis and cell cycle redistribution

LIJUN HU[*], FEI SUN[*], ZHIQIANG SUN, XINCHU NI, JIAN WANG, JIANLIN WANG, MENGYUN ZHOU, YUE FENG, ZE KONG, QIU HUA and JINGPING YU

Department of Radiation Oncology, The Second People's Hospital of Changzhou, Nanjing Medical University, Changzhou, Jiangsu 213003, P.R. China

**Abstract.** To determine the radiosensitizing effect of apatinib on esophageal cancer cells, and to preliminarily investigate the underlying mechanism, KYSE-150 cells were treated with apatinib, x-ray or apatinib combined with x-ray, and compared with a blank control. It was observed that apatinib significantly inhibited vascular endothelial growth factor (VEGF) secretion and the proliferation of KYSE-150 cells in a dose-dependent manner. As the concentration of apatinib increased, the radiobiological parameters inactivation dose ($D_0$), quasi domain does ($D_q$) and survival fraction ($SF_2$) of KYSE-150 cells decreased, while the sensitization enhancement ratio $SER_{D0}$ increased. The rate of apoptosis in cells treated with apatinib and x-ray was markedly higher compared with those of the blank control, x-ray and apatinib alone groups (P<0.05). The proportion of cells in the G2/M phase was significantly increased in the apatinib, x-ray and combination groups compared with the blank control group (P<0.05). Compared with the control and x-ray groups, combination treatment did not significantly alter the expression level of polyADP-ribose polymerase (PARP), although it significantly increased the expression of cleaved-PARP (P<0.05). Moreover, the expression of cell serine/threonine-protein kinase-2 (CHK2) was downregulated (P<0.05), whilst expression of the phosphorylated form, pCHK2, was significantly increased (P<0.05) in the combination group when compared with the control and x-ray groups. In conclusion, the present study suggested that apatinib

increases the radiosensitivity of KYSE-150 esophageal cancer cells by inhibiting VEGF secretion and cell proliferation, and promoting apoptosis and cell cycle redistribution.

## Introduction

China has a high incidence of esophageal cancer; as the third most common cancer in men, and the fifth in women, the disease ranks fourth for mortality rate among malignant tumors, regardless of sex (1). The most common type of esophageal cancer is squamous cell carcinoma (SCC), accounting for >90% of cases. Radiation therapy is one of the principal treatments for advanced esophageal cancer, although treatment efficacy remains unsatisfactory. Although radiotherapy has markedly improved, in addition to combination treatment with chemotherapy and radiotherapy, the 5-year survival rate of patients with local advanced esophageal SCC treated with concurrent radiation therapy and chemotherapy is only 23-34% (2). The local recurrence of lesions within the radiation field caused by radiation resistance is a primary cause of treatment failure, accounting for ~50% of cases (2). Therefore, enhancing the radiosensitivity of esophageal cancer cells may improve the success rate of radiotherapy, and reduce local recurrence of esophageal cancer following radiotherapy.

A principle cause of radioresistance in esophageal cancer is the abnormal secretion of radiation-induced vascular endothelial growth factor (VEGF), which contributes to tumor angiogenesis and protects tumor vessels from radiation-associated damage. Studies have revealed that the expression of VEGF is closely associated with tumor vascular invasion, lymph node metastasis and poor prognosis (3,4). VEGF binds to the vascular endothelial growth factor receptor (VEGF-R) on the endothelial cell membrane to initiate tumor angiogenesis, and ultimately results in angiogenesis and lymphangiogenesis, and subsequent radioresistance (4,5).

Apatinib (YN968D1) is a small molecule tyrosine kinase inhibitor that selectively inhibits the activity of VEGFR-2, blocking signal transduction following binding to VEGF. This inhibits the proliferation and migration of endothelial cells, thereby inhibiting tumor angiogenesis (6). It is indicated that apatinib is a VEGF inhibitor with the potential to reverse the

radioresistance of esophageal cancer cells. However, whether concurrent radiotherapy and apatinib is useful for the treatment of esophageal cancer, and its underlying mechanism of action, remains to be identified. Therefore, the present study investigated the effects of apatinib on esophageal squamous cell carcinoma and its impact on the radiosensitivity of the cancer cells, using the human cell line KYSE-150; a potential mechanism of action was also explored. The present study aimed to provide guidance for apatinib use in enhancing the success rate of radiotherapy and reducing local recurrence, in addition to improving the prognosis of patients with esophageal SCC.

**Materials and methods**

*Reagents and equipment*. RPMI 1640 culture medium (containing 0.25% EDTA), trypsin, penicillin and streptomycin was purchased from Gibco (Thermo Fisher Scientific, Inc., Waltham, MA, USA), and diluted prior to experimentation. Fetal bovine serum was purchased from Hangzhou Sijiqing Biological Engineering Materials Co., Ltd., (Hangzhou, China). Apatinib solution at a concentration of 10 mmol/l was purchased from MedChemExpress (Monmouth Junction, NJ, USA). The human VEGF ELISA kit was purchased from NeoBioscience Technology Co., Ltd., (Shenzen, China; catalog no. EHC-108.96). The Cell Counting Kit-8 (CCK-8) kit was purchased from Dojindo Molecular Technologies, Inc., (Kumamoto, Japan). Crystal violet staining solution, the Annexin V-fluorescein isothiocyanate (FITC) apoptosis detection kit, and the cell cycle and apoptosis detection kits were purchased from Beyotime Institute of Biotechnology (Jiangsu, China). The Primus-H medical linear accelerator (Siemens AG, Munich, Germany) was used for x-ray irradiation, with an absorbed dose rate of 1 Gy/min at 100 cm distance between the source and the target. The flow cytometer was purchased from BD Biosciences (San Jose, CA, USA).

*Cell lines and culture*. The human esophageal squamous cell carcinoma cell line KYSE-150 was purchased from the Cell Bank of Type Culture Collection of Chinese Academy of Sciences (Shanghai, China; cat. no; TCHu230) and cultured in RPMI 1640 medium supplemented with 10% fetal bovine serum and 1% penicillin/streptomycin, in a 37°C incubator with 5% $CO_2$; cells were passaged every 2-3 days. Cells in the exponential growth phase were used for the experiment.

*ELISA for VEGF secretion*. Experimental groupings were as follows: Blank control, x-ray (6 Gy), apatinib (10 and 20 $\mu$mol/l), and apatinib combined with x-ray. The cells in each group were collected following x-ray treatment and cultured in fresh medium for 24 h. Supernatants were collected and 100 $\mu$l (200 pg/ml) was added to each ELISA plate coated with a VEGF monoclonal antibody. The detection was performed according to the manufacturer's protocol. The concentration of VEGF in the supernatant was calculated according to the absorbance of the specimen, which was determined using a microplate reader at a wavelength of 450 nm.

*Cell proliferation assay*. Cells in the exponential growth phase were digested with trypsin and resuspended. A total of 5,000 cells were seeded into each well of a 96-well culture plate. Following 24 h, the culture medium in the apatinib group was replaced with 200 $\mu$l medium containing apatinib at concentrations of 5, 10, 20, 30 and 40 $\mu$mol/l. The cells of the blank control group were cultured in complete medium without apatinib. Each group contained six parallel wells. The plate was incubated in a 37°C incubator containing 5% $CO_2$ for 24, 48 and 72 h. Following treatment, 10 $\mu$l of CCK-8 solution was added to each well, and the plate was further cultured for 4 h. The absorbance (A) at 450 nm was measured and the proliferation inhibition rate was calculated [cell proliferation inhibition rate (%) = 1-(A value of experimental group-A value of blank group)/(A value of control group-A value of blank group) x100%]. The half-maximal inhibitory concentration ($IC_{50}$) was calculated. Each experiment was repeated three times independently.

*Colony formation assay*. The experiment included the control, x-ray (2, 4, 6, and 8 Gy), apatinib (10, 20 and 40 $\mu$mol/l) and combination groups (with the same apatinib concentrations as in the apatinib group and the same x-ray doses as in the x-ray group). Cells were seeded in 60x60 mm cell culture dishes at 500 cells/dish. Following incubation for 24 h, the medium in the apatinib and combination groups was replaced with fresh medium containing 10, 20 and 40 $\mu$mol/l apatinib. The cells were incubated for an additional 48 h, followed by x-ray irradiation. Following irradiation, the medium was replaced with fresh culture medium without apatinib and incubated for 8 days. The colonies were washed with PBS, fixed with 4% paraformaldehyde a room temperature for 15 min, and stained with crystal violet at room temperature for 5 min. The colonies consisting of ≥50 cells were counted under a microscope and the colony formation rate (%) was calculated as follows: number of colonies counted/number of cells seeded x100%. The surviving fraction (SF) was determined as follows: SF = number of colonies/number of cells seeded under the same condition x colony formation rate. The cell survival curves were fitted by multi-target model $SF = 1-(1-e^{-D/D0})^N$, the radiological parameters, including the extrapolation number (N), inactivation does ($D_0$), quasi domain dose ($D_q$) and survival rate ($SF_2$) were determined, and the radiosensitization ratio was calculated. All experiments were repeated three times independently.

*Cell cycle analysis*. The experimental groups included the blank control, x-ray (4 Gy), apatinib (20 $\mu$mol/l) and apatinib combined with x-ray groups. The cell culture and apatinib treatment duration were the same as those in the colony formation assay. Following x-ray irradiation, the cells were cultured in fresh medium for 24 h, trypsinized, and centrifuged at 106 x g for 5 min. Cells were washed with PBS and fixed in 75% ethanol at 4°C overnight. Ethanol was the removed by centrifugation at 106 x g for 5 min. The cells were washed with PBS and resuspended in propidium iodide (PI) solution containing RNase (1.87%), incubated at 37°C in the dark for 30 min, and analyzed with a flow cytometer. FlowJo 7.6 software (FlowJo LLC, Ashland, OR, USA) was used to calculate the cell cycle distribution. Each experiment was repeated three times independently.
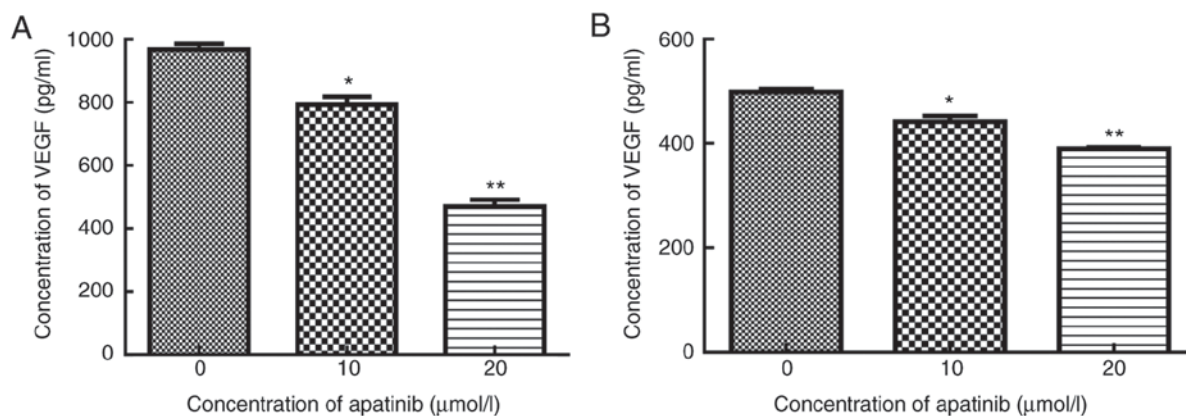
Figure 1. Apatinib inhibits VEGF secretion in KYSE-150 cells. KYSE-150 cells were irradiated with (A) 0 Gy and (B) 6 Gy x-ray following treatment with different concentrations of apatinib for 48 h. The VEGF concentration was calculated by ELISA, which indicated that the secretion of VEGF was significantly decreased in apatinib-treated KYSE-150 cells. All data are presented as the mean ± standard deviation, from three independent experiments. *P<0.05; **P<0.01 vs. control. VEGF, vascular endothelial growth factor.

*Detection of apoptosis using the Annexin V-FITC assay.* Cells were divided into the same four groups as described above. The cells were incubated for 24 h after a change of the medium following x-ray irradiation. The cells were trypsinized and counted under a light microscope (magnification, x40). The cell suspensions were stained at a density of $1x10^6$ cells/ml using the Annexin V-FITC Apoptosis detection kit, as per the manufacturer's protocol; subsequent flow cytometric analysis was performed. The apoptosis rate was analyzed using FlowJo software. All experiments were repeated three times independently.

*Western blot analysis.* Experimental groupings were as described above. Cell inoculation, treatment with apatinib and x-ray irradiation were the same as those in the above experiments. Following x-ray irradiation, the cells were cultured for 24 h. The protein was extracted from the cells with radioimmunoprecipitation assay buffer and quantified using a BCA kit (catalog no. P0011; Beyotime Institute of Biotechnology). A total of 30 $\mu$g protein was loaded per lane for western blot analysis. 10% SDS-PAGE and 5% stacking gels were prepared, and the protein samples were electrophoresed. The proteins were then transferred to a polyvinyl difluoride membrane (catalog no. IPVH00010; EMD Millipore, Billerica, MA, USA) and blocked with TBS and Tween-20 (Sangon Biotech Co., Ltd., Shanghai, China) with 5% skim milk for 1 h at room temperature. The membranes were then incubated with the following primary antibodies: Anti-PARP/cleaved-PARP (catalog no. 9915; 1:1,000; Cell Signaling Technology, Inc., Danvers, MA, USA); anti-phospho-serine/threonine-protein kinase-2 (pCHK2; catalog no. 9917; 1:1,000; Cell Signaling Technology, Inc.); and anti-VEGFR-2 (catalog no. 2472; 1:1,000; Cell Signaling Technology, Inc.) at 4°C overnight. Subsequently, the membranes were incubated with anti-rabbit IgG, horseradish peroxidase-linked secondary antibody (catalog no. 9915; 1:1,000; Cell Signaling Technology, Inc) for 1.5 h at room temperature. Visualization was performed with enhanced chemiluminescence reagent (catalog no. 32106; Thermo Fisher Scientific, Inc.). Image J 1.8.0 processing software (Bio-Rad Laboratories, Inc., Hercules, CA, USA) was used for gray-scale analysis. Anti-GAPDH (catalog no. 5174; 1:1,000; Cell
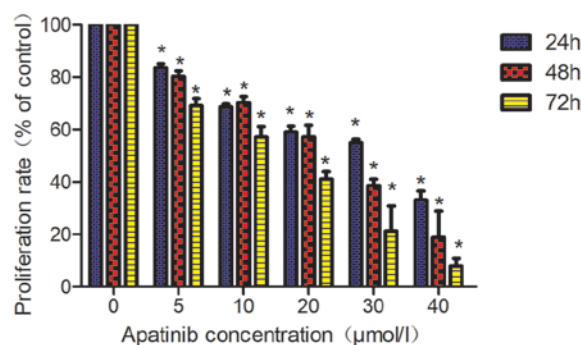


Figure 2. Apatinib inhibits the proliferation rate of KYSE-150 cells. KYSE-150 cells were treated with various concentrations of apatinib (0, 5, 10, 20, 30 and 40 $\mu$mol/l) for 24, 48 and 72 h. Cell proliferation rate was calculated using a Cell Counting Kit-8 assay. Apatinib significantly inhibited the proliferation rate of KYSE-150 cells in a time- and dose-dependent manner. All data are presented as the mean ± standard deviation from three independent experiments. *P<0.05 vs. corresponding control.

Signaling Technology, Inc.) was used as an internal reference. Each experiment was repeated three times independently.

*Statistical analysis.* All data are expressed as the mean ± standard deviation. SPSS version 20.0 was used for the statistical analyses (IBM Corp., Armonk, NY, USA). For comparisons between two groups, the Student's t-test was used. One-way analysis of variance was used for comparisons between ≥2 groups, followed by the Student-Newman-Keuls test when equal variance was assumed, and Dunnett's T3 test when equal variance was not assumed. Liner-regression analysis was used to analyze the cell proliferation rate. Radiation survival curves were fitted according to the single hit, multi-target equation (7). P<0.05 was considered to indicate a statistically significant difference.

**Results**

*Apatinib inhibits VEGF secretion in KYSE-150 cells in a dose-dependent manner.* To evaluate the impact of apatinib on VEGF secretion in KYSE-150 cells, the cells were treated

Table I. Cell proliferation inhibition rate in KYSE-150 cells treated with different concentrations of apatinib (%; mean ± standard deviation).

| Apatinib concentration ($\mu$mol/l) | Treatment duration | | |
|---|---|---|---|
| | 24 h | 48 h | 72 h |
| 0 | 0 | 0 | 0 |
| 5 | 16.40±1.56[a] | 19.72±2.04[a] | 31.00±2.87[a,c] |
| 10 | 31.37±1.10[a] | 29.69±2.28[a] | 43.00±4.12[a,c] |
| 20 | 40.92±2.20[a] | 42.84±4.48[a] | 59.00±2.91[a,c] |
| 30 | 45.08±1.29[a] | 61.38±2.45[a,b] | 78.79±9.60[a,c] |
| 40 | 67.00±3.58[a] | 81.23±10.08[a] | 92.06±2.82[a,b] |

[a]$P<0.05$ vs. respective 0 $\mu$mol/l group; [b]$P<0.05$ vs. respective 24 h group of the same concentration; [c]$P<0.05$ vs. respective 48 h group of the same concentration.

with varying doses of apatinib and the level of VEGF secretion determined by ELISA. In cells treated with 10 and 20 $\mu$mol/l apatinib, the levels of VEGF were 792.6±27.10 and 469.6±22.58 pg/ml, respectively, which were significantly lower compared with that of the control group, 969.1±7.44 pg/ml ($P<0.05$). VEGF level was even lower in cells treated with the combination of apatinib and x-ray. In cells treated with x-ray and 10 or 20 $\mu$mol/l apatinib, the levels of secreted VEGF were 441.3±11.43 and 390.2±15.54 pg/ml, respectively, significantly lower compared with that of the x-ray group, 498.8±15.81 pg/ml (t=4.44, 17.12, $P<0.05$). As illustrated in Fig. 1, Apatinib inhibited VEGF secretion in KYSE-150 cells in a dose-dependent manner ($r^2$=0.96-0.97; $P<0.05$).

*Apatinib inhibits the proliferation rate of KYSE-150 cells in a dose- and time-dependent manner.* The proliferation rate of KYSE-150 cells was determined using the CCK-8 assay. With an increase in apatinib concentration and treatment time, the cell proliferation rate of KYSE-150 cells decreased significantly (Fig. 2; Table I). The IC50 values for apatinib in KYSE-150 cells treated for 24, 48 and 72 h were 26.53±0.61, 18.86±0.42, and 11.15±0.26 $\mu$mol/l, respectively, suggesting that the inhibitory effect was dose- and time-dependent ($r^2$=0.89-0.96; $P<0.05$). Based on these findings, KYSE-150 cells were treated with 10, 20 and 40 $\mu$mol/l apatinib for 48 h to further analyze the impact of apatinib on the radiosensitivity of KYSE-150 cells.

*Apatinib enhances the radiosensitivity of KYSE-150 cells.* To determine whether apatinib acts as a radiosensitizer, KYSE-150 cells were treated with apatinib for 48 h prior to irradiation (2-8 Gy). The radiosensitivity of the cells was evaluated by the clone formation assay. The survival fraction of KYSE-150 cells decreased with an increase in radiation dose (Fig. 3). Compared with the control group, the higher the concentration of apatinib, the lower the survival fraction of the cells following x-ray irradiation. Sensitization enhancement ratios (SER) revealed that in cells treated with 20 and 40 $\mu$mol/l apatinib, the $SER_{D0}$ were 1.36 and 1.36, respectively, and $SER_{Dq}$ were 1.35 and 2.96, respectively. The radiobiological parameters ($D_0$, $D_q$ and $SF_2$ values) of KYSE-150
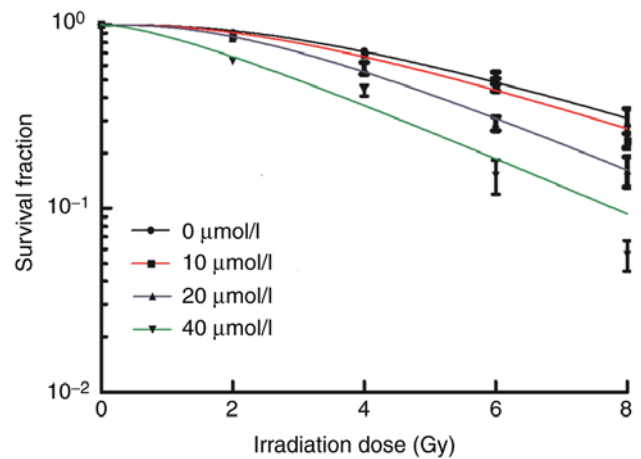


Figure 3. Survival fraction of KYSE-150 cells pretreated with apatinib, followed by irradiation. Apatinib remarkably increased the radiosensitivity of KYSE-150 cells, with SERD0 of 1.36 for 20 and 40 $\mu$mol/l apatinib. All data are presented as the mean ± standard deviation from three independent experiments.

decreased with increased concentrations of apatinib (Table II). These results indicated that apatinib enhanced the sensitivity of KYSE-150 cells to x-ray irradiation.

*Apatinib enhances radiation-induced apoptosis in KYSE-150 cells.* To investigate the mechanism by which apatinib increased the radiosensitivity of KYSE-150 cells, cells were pretreated with 20 $\mu$mol/l apatinib for 48 h prior to x-ray irradiation at 4 Gy. Apoptosis was determined using the Annexin V/PI assay. The apoptosis rates of the apatinib, x-ray, and the combination of apatinib and x-ray groups were 15.65±1.54, 8.30±1.18 and 19.70±1.66% respectively, which were significantly higher compared with that of the control group (3.49±0.74%) (Fig. 4). To further investigate the mechanism through which apatinib induces apoptosis, the expression of poly (ADP-ribose) polymerase PARP and cleaved-PARP in KYSE-150 cells was examined. It was indicted that the level of cleaved-PARP was markedly increased in the combination group compared with those of the control and x-ray groups,

Table II. Radiosensitization effects of apatinib in KYSEe-150 cells *in vitro*.

| Apatinib concentration ($\mu$mol/l) | $D_0$ | $D_q$ | $SF_2$ | $SER_{D0}$ | $SER_{Dq}$ |
|---|---|---|---|---|---|
| 0 | 3.79±0.69 | 4.06±0.27 | 0.90±.019 | 1±0 | 1±0 |
| 10 | 3.60±0.41 | 3.66±0.22 | 0.87±0.02 | 1.05±0.20 | 1.11±0.10 |
| 20 | 2.83±0.34[a] | 3.00±0.13[a] | 0.84±0.03 | 1.36±0.36[a] | 1.35±0.11[a] |
| 40 | 2.81±0.17[a] | 1.38±0.23[a] | 0.66±0.02[a] | 1.36±0.27[a] | 2.96±0.30[a] |

All data are presented as the mean ± standard deviation from three independent experiments. Compared with the same index sample treated with 0 $\mu$mol/l apatinib, [a]P<0.05 vs. respective 0 $\mu$mol/l group. $D_0$, inactivation dose; Dq, quasi domain dose; $SF_2$, surviving fraction of 2 Gy; SER, sensitization enhancement ratio.

though the expression of PARP was not markedly altered, demonstrating that apatinib enhances PARP-mediated apoptosis in KYSE-150 cells (Fig. 5).

*Apatinib accelerates radiation-induced cell cycle redistribution and causes G2/M-phase arrest in KYSE-150 cells.* To further identify the mechanism underlying the radiosensitization effect of apatinib, the cell cycle distribution of KYSE-150 cells was analyzed by PI staining. As illustrated in Fig. 6, the proportions of cells in the G2/M phase within the apatinib, x-ray and combination groups were 26.27±3.30, 68.79±2.77 and 47.27±3.59% respectively, significantly higher compared with that of the control group (12.14±2.13%). The expression of pCHK2, an important G2/M phase checkpoint protein and a central signaling molecule of the DNA damage response, was markedly higher in the combination group compared with that in the control and apatinib group (Fig. 7). By contrast, the expression of pCHK2 in the combination group was lower compared with that in x-ray alone group. This indicated that apatinib may not only increase the population of KYSE-150 cells in the G2/M phase, but may also inhibit the DNA repair response (Fig. 6). Data was not shown regarding the influence of Apatinib on VEGFR-2 expression in KYSE-150 cells.

## Discussion

High expression of VEGF is one of the primary causes of radioresistance in esophageal cancer cells. Studies have revealed that combination treatment with radiotherapy and anti-VEGF compounds significantly reduces the radioresistance of esophageal cancer cells and tissues, thereby enhancing radiosensitivity (4). In order to investigate the specific mechanism through which anti-VEGF drugs reduce radioresistance, the effects of apatinib, a new molecular-targeted compound, was investigated in combination with radiotherapy for its ability to alter the radiosensitivity of esophageal cancer cells *in vitro*.

Apatinib is a small molecule tyrosine kinase inhibitor that targets VEGFR-2. The inhibitory effects of apatinib have been reported in a number of human cancer types including colon cancer, leukemia and intrahepatic bile duct cancer, wherein apatinib acts to promote apoptosis and increase the sensitivity of cancer cells to chemotherapy (8-10). However, little is known about the effects of apatinib on the radiosensitization of tumor cells, and its corresponding mechanism of action. In the present study, analysis of the phosphorylation level of VEGFR-2 was attempted by western blotting, however, this was unsuccessful. A previous study suggested that VEGFR-2 expression relies on vascular endothelial cells, and that experiments in vitro may be unable to detect VEGFR-2 expression (11). As a result, no further experiments with VEGFR-2 were conducted in the present study. VEGF is the upstream ligand of VEGFR-2, and it was observed that apatinib significantly reduced the secretion of VEGF in KYSE-150 esophageal cancer cells in a concentration-dependent manner; this suggests that apatinib may have a potential radiosensitization effect on these cells. Subsequently, a series of experiments were conducted to determine the radiosensitization effects of apatinib in KYSE-150 cells, and its potential mechanism of action. It was indicated that apatinib significantly inhibited the proliferation of KYSE-150 cells in a dose- and time-dependent manner. Compared with 24 and 48 h treatment, the inhibitory effects of a 72 h treatment with apatinib were markedly increased, suggesting that apatinib acts in a time-dependent manner in KYSE-150 cells. The survival fraction of KYSE-150 cells decreased exponentially with increasing radiation exposure. The radiobiological parameters $D_0$, $D_q$ and $SF_2$ of KYSE-150 cells gradually decreased with increasing concentrations of apatinib, whereas the radiosensitization ratio $SER_{D0}$ of the cells increased; the higher the radiosensitization ratio, the higher the radiosensitivity. The results suggested that apatinib increases the radiosensitivity of KYSE-150 cells by inhibiting the repair of sublethal cell damage.

Ionizing radiation-induced cell killing is predominantly associated with DNA double-strand breaks (DSBs) and cell cycle redistribution. Apoptosis is regulated by a series of signaling pathways, including the caspase-9/caspase-3/PARP pathway (10). Pro-apoptotic signaling promotes the relocation of cytochrome c oxidase from the mitochondria to the cytoplasm, and activates cytoplasmic caspase-9, which cleaves and activates downstream proteins such as caspase-3 (8). Activated caspase-3 cleaves PARP, which consequently causes the separation of two catalytic domains at the PARP-carboxy terminus, and a subsequent reduction in function, which leads to DNA fragmentation and the induction of apoptosis (8). Studies have suggested that apoptosis is associated with the radiosensitivity of cells, and the extent of apoptosis may be used as a measure of radiosensitivity (9).
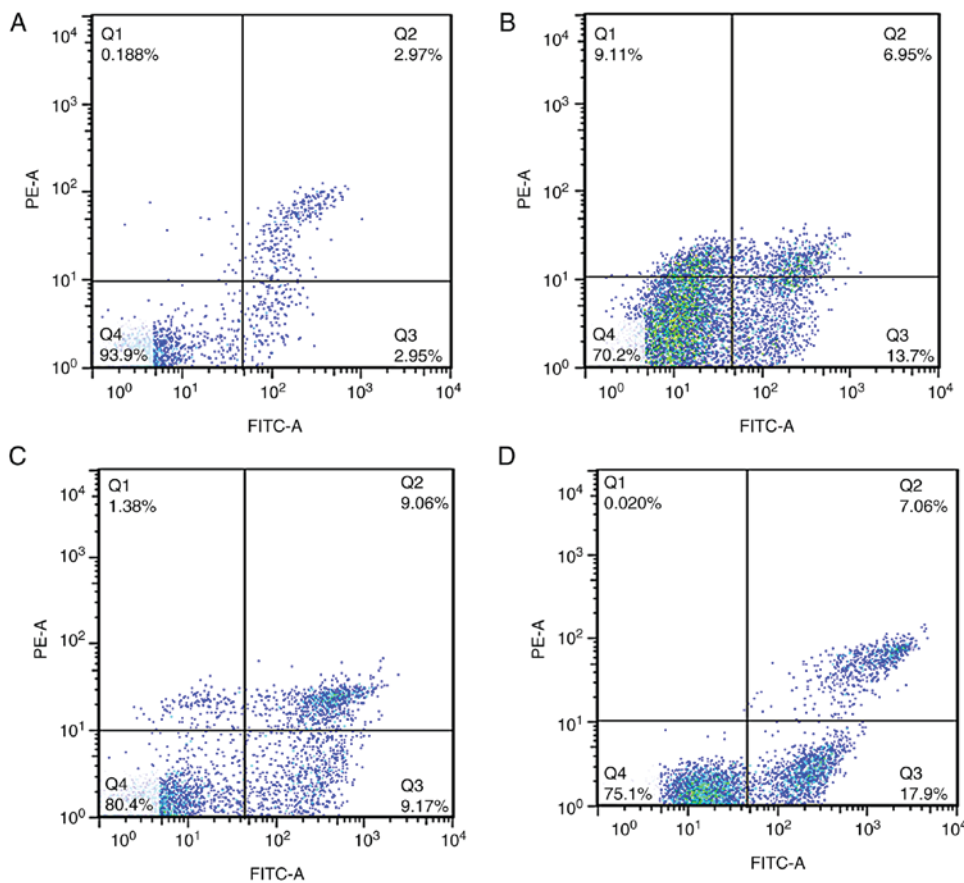
Figure 4. Effects of apatinib combined with x-ray iradiation on apoptosis in KYSE-150 cells. KYSE-150 cells were pretreated with 20 $\mu$mol/l apatinib for 48 h prior to irradiation (4 Gy). Following irradiation, the cells were further incubated for 24 h. The apoptosis rate of the cells was analyzed by Annexin V/PI staining and flow cytometry. The apoptosis rates of the apatinib, x-ray and apatinib combined with x-ray groups were higher compared with that of the control group. Representative images of flow cytometric analysis are presented as follows: (A) Control group; (B) apatinib group; (C) radiation alone group; (D) combination group. All data are presented as the mean ± standard deviation from three independent experiments. PI, propidium iodide; FITC, fluorescein isothiocyanate; PI, propidium iodide; Q, quadrant.
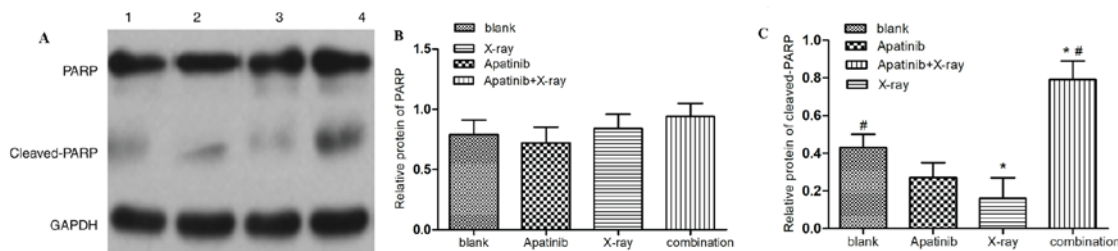


Figure 5. Effects of apatinib and x-ray on the expression of PARP and cleaved-PARP in KYSE-150 cells. (A) The protein levels of PARP and cleaved-PARP were determined by western blotting. Lane 1, control group; lane 2, apatinib group; lane 3, x-ray group; and lane 4, combination group. (B) Quantitative analysis of the protein expression of PARP. (C) Quantitative analysis of the protein expression of cleaved-PARP. All data are presented as the mean ± standard deviation from three independent experiments. *P<0.05 vs. blank group. #P<0.05 vs. the same index sample treated with 4 Gy x-ray. PARP, poly (ADP-ribose) polymerase.

In the present study, it was found that apatinib and x-ray promote the apoptosis of esophageal cancer cells, although the apoptotic effect of combination treatment was markedly higher compared with that of apatinib or x-ray alone. Western blotting results further confirmed that apatinib increased the cleavage and inactivation of the apoptosis-regulatory protein PARP, accelerating radiation-induced apoptosis. The exact apoptosis regulatory signaling pathway in esophageal cancer cells remains unclear, and further research is required for clarification.

Following irradiation, cancer cells activate DNA damage response pathways to repair DSBs. Furthermore, cell cycle checkpoints remove damaged cells from the actively proliferating population, and halt the cell cycle to temporarily allow for the repair of DSBs, another primary reason for radioresistance in cancer cells (12). CHK2 is a key kinase in this signaling pathway and is an important checkpoint protein of the G2/M phase. Its activation promotes the repair of DNA damage and prevents the entry of DNA into mitosis (13). It is therefore a key target in radiobiology. The present study
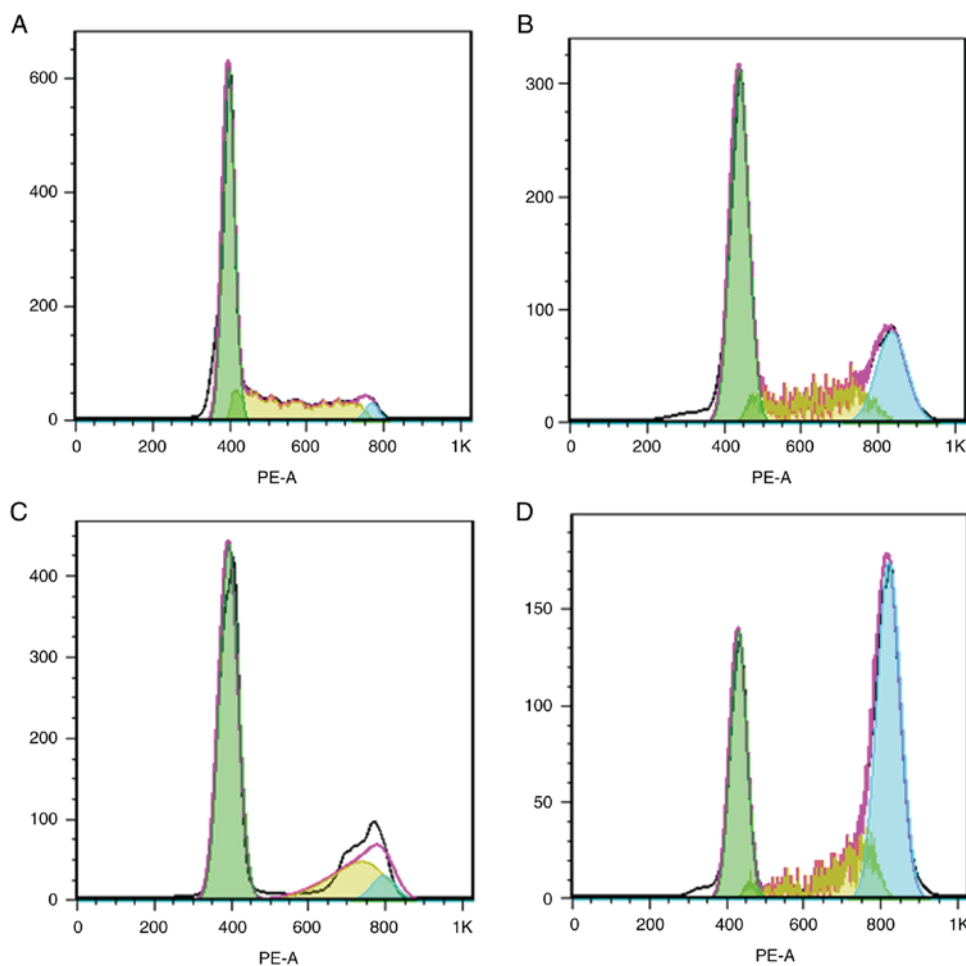
Figure 6. Effect of combination treatment of apatinib and x-ray irradiation on cell cycle distribution in KYSE-150 cells. KYSE-150 cells were pretreated with 20 $\mu$mol/l apatinib for 48 h prior to being exposed to 4 Gy radiation. The cells were incubated for another 24 h following irradiation and cell cycle distribution in the cells was analyzed by flow cytometry. The proportions of cells in the G2/M phase in the apatinib, x-ray and apatinib combined with x-ray groups were significantly higher compared with that of the control group. Representative images of flow cytometric analysis were presented as follows: (A) Control group; (B) apatinib group; (C) radiation alone group; (D) combination group. All data are presented as the mean ± standard deviation from three independent experiments. PE, phycoerythrin.
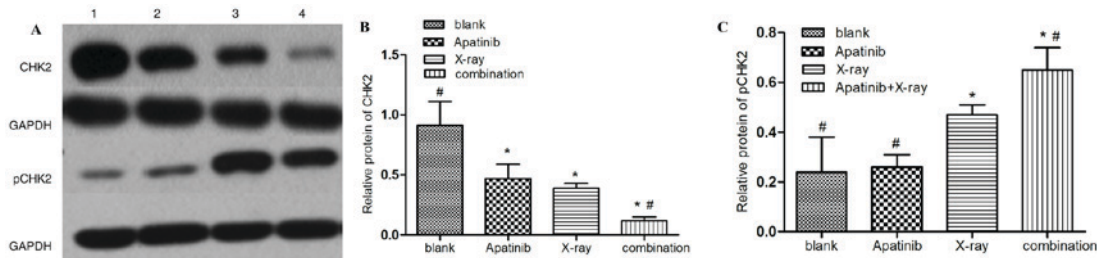


Figure 7. Effects of apatinib and x-ray on the expression of CHK2 and pCHK2 in KYSE-150 cells. (A) The protein levels of CHK2 and pCHK2 were determined by western blotting. Lane 1, control group; lane 2, apatinib group; lane 3, x-ray group; and lane 4, combination group. (B) Quantitative analysis of the protein expression of CHK2. (C) Quantitative analysis of the protein expression of pCHK2. All data are presented as the mean ± standard deviation from three independent experiments. *$P<0.05$ vs. blank group. #$P<0.05$ vs. the same index sample treated with 4 Gy x-ray. CHK2, serine/threonine-protein kinase-2; p, phosphorylated.

illustrated that following x-ray irradiation, the proportion of cells in the G2/M phase was significantly increased, and pretreatment with apatinib prior to irradiation significantly increased radiation-induced G2/M arrest. Meanwhile, apatinib considerably downregulated the radiation-induced phosphorylation of CHK2. This further confirmed that apatinib promotes cell cycle arrest in esophageal cancer cells by inhibiting CHK2

and through the subsequent repair of DNA damage, thereby accelerating apoptosis.

Apatinib is a novel drug developed in China, which has been widely used for the treatment of advanced gastric cancer, colorectal cancer, non-small cell lung cancer and breast cancer (10,14,15). However, its specific mechanism of action and target when combined with radiotherapy remain unclear.

In the present study, it was demonstrated that apatinib markedly increased radiosensitivity by inhibiting the secretion of VEGF and the proliferation of KYSE-150 cells. When combined with x-ray irradiation, apatinib markedly inhibited cancer cell survival, and induced apoptosis by activating PARP-mediated apoptotic signaling pathways and cell cycle redistribution, which corresponded to the reduced level of pCHK2. Therefore an association between VEGF and CHK2 is hypothesized, although the specific mechanism is unclear. This provides scope for further studies on the radiosensitizing mechanism of apatinib for the treatment of esophageal cancer, and provides a theoretical basis for novel strategies for esophageal cancer combination therapy. As a small molecular tyrosine kinase inhibitor, it is also important to verify the effects of apatinib on the expression level of the receptor tyrosine kinase c-Kit, and the proto-oncogene tyrosine-protein kinase c-SRC, which is a limitation of the present study that requires further investigation.

## Acknowledgements

## Availability of data and materials

The datasets used and/or analyzed during the current study are available from the corresponding author on reasonable request.

## Authors' contributions

FS conducted the majority of the experiments; ZS, SN and JW assisted with the experiments; LH and JW conducted statistical analysis and guided the research process; LH drafted the manuscript and proposed revision suggestions; MZ, YF, ZK and QH assisted in the completion of experiments; JY participated in the development of the research idea and experimental design, and proposed revision suggestions.

## Ethics approval and consent to participate

Not applicable.

## Patient consent for publication

Not applicable.

## Competing interests

The authors declare that they have no competing interests.

## References

1. Chen W, Zheng R, Baade PD, Zhang S, Zeng H, Bray F, Jemal A, Yu XQ and He J: Cancer statistics in China, 2015. CA Cancer J Clin 66: 115-132, 2016.
2. Welsh J, Settle SH, Amini A, Xiao L, Suzuki A, Hayashi Y, Hofstetter W, Komaki R, Liao Z and Ajani JA: Failure patterns in patients with esophageal cancer treated with definitive chemo-radiation. Cancer 118: 2632-2640, 2012.
3. Cellini F and Valentini V: Targeted therapies in combination with radiotherapy in oesophageal and gastroesophageal carcinoma. Curr Med Chem 21: 990-1004, 2014.
4. Yu J, Liu F, Sun Z, Sun M and Sun S: The enhancement of radiosensitivity in human esophageal carcinoma cells by thalidomide and its potential mechanism. Cancer Biother Radiopharm 26: 219-227, 2011.
5. Yu JP, Sun SP, Sun ZQ, Ni XC, Wang J, Li Y, Hu LJ and Li DQ: Clinical trial of thalidomide combined with radiotherapy in patients with esophageal cancer. World J Gastroenterol 20: 5098-5103, 2014.
6. Tian S, Quan H, Xie C, Guo H, Lu F, Xu Y, Li J and Lou L: YN968D1 is a novel and selective inhibitor of vascular endothelial growth factor receptor-2 tyrosine kinase with potent activity in vitro and in vivo. Cancer Sci 102: 1374-1380, 2011.
7. Leith JT, Davis PJ, Mousa SA and Hercbergs AA: In vitro effects of tetraiodothyroacetic acid combined with X-irradiation on basal cell carcinoma cells. Cell Cycle 16: 367-373, 2017.
8. Ghorai A, Sarma A, Bhattacharyya NP and Ghosh U: Carbon ion beam triggers both caspase-dependent and caspase-independent pathway of apoptosis in HeLa and status of PARP-1 controls intensity of apoptosis. Apoptosis 20: 562-580, 2015.
9. Rahmanian N, Hosseinimehr SJ and Khalaj A: The paradox role of caspase cascade in ionizing radiation therapy. J Biomed Sci 23: 88, 2016.
10. Lin Y, Zhai E, Liao B, Xu L, Zhang X, Peng S, He Y, Cai S, Zeng Z and Chen M: Autocrine VEGF signaling promotes cell proliferation through a PLC-dependent pathway and modulates apatinib treatment efficacy in gastric cancer. Oncotarget 8: 11990-12002, 2017.
11. Lin YC, Liu CY, Kannagi R and Yang RB: Inhibition of endothelial SCUBE2 (Signal Peptide-CUB-EGF Domain-Containing Protein 2), a novel VEGFR2 (Vascular Endothelial Growth Factor Receptor 2) coreceptor, suppresses tumor angiogenesis. Arterioscler Thromb Vasc Biol 38: 1202-1215, 2018.
12. Morgan MA and Lawrence TS: Molecular pathways: Overcoming radiation resistance by targeting DNA damage response pathways. Clin Cancer Res 21: 2898-2904, 2015.
13. Manic G, Obrist F, Sistigu A and Vitale I: Trial watch: Targeting atm-chk2 and atr-chk1 pathways for anticancer therapy. Mol Cell Oncol 2: e1012976, 2015.
14. Zhou N, Liu C, Hou H, Zhang C, Liu D, Wang G, Liu K, Zhu J, Lv H, Li T and Zhang X: Response to apatinib in chemotherapy-failed advanced spindle cell breast carcinoma. Oncotarget 7: 72373-72379, 2016.
15. Song Z, Yu X, Lou G, Shi X and Zhang Y: Salvage treatment with apatinib for advanced non-small-cell lung cancer. Onco Targets Ther 10: 1821-1825, 2017.